Available online at www.sciencedirect.com
SCIENCE DIRECT®
Bioorganic & Medicinal Chemistry 13 (2005) 2825–2836
Bioorganic & Medicinal Chemistry

Targeting the gatekeeper residue in phosphoinositide 3-kinases

Peter J. Alaimo,[a,†] Zachary A. Knight[b,†] and Kevan M. Shokat[a,c,*]

[a]*Department of Cellular and Molecular Pharmacology, University of California, San Francisco, CA 94143-2280, USA*
[b]*Program in Chemistry and Chemical Biology, University of California, San Francisco, CA 94143, USA*
[c]*Department of Chemistry, University of California, Berkeley, CA 94720, USA*

Received 1 December 2004; accepted 12 February 2005

Abstract—A single residue in the ATP binding pocket of protein kinases—termed the gatekeeper—has been shown to control sensitivity to a wide range of small molecule inhibitors (*Chem. Biol.* **2004**, *11*, 691; *Chem. Biol.* **1999**, *6*, 671). Kinases that possess a small side chain at this position (Thr, Ala, or Gly) are readily targeted by structurally diverse classes of inhibitors, whereas kinases that possess a larger residue at this position are broadly resistant. Recently, lipid kinases of the phosphoinositide 3-kinase (PI3-K) family have become the focus of intense research interest as potential drug targets (*Chem. Biol.* **2003**, *10*, 207; *Curr. Opin. Pharmacol.* **2003**, *3*, 426). In this study, we identify the residue that corresponds structurally to the gatekeeper in PI3-Ks, and explore its importance in controlling enzyme activity and small molecule sensitivity. Isoleucine 848 of p110α was mutated to alanine and glycine, but the mutated kinase was found to have severely impaired enzymatic activity. A structural bioinformatic comparison of this kinase with its yeast orthologs identified second site mutations that rescued the enzymatic activity of the I848A kinase. To probe the dimensions of the gatekeeper pocket, a focused panel of analogs of the PI3-K inhibitor LY294002 was synthesized and its activity against gatekeeper mutated and wild-type p110α was assessed.

1. Introduction

In the past decade protein kinases have emerged as one of the most important new classes of drug targets. Protein kinases play a central role in many signaling pathways disregulated in disease, and these enzymes can be readily targeted with cell permeable, small molecule inhibitors.[5] These facts have led to the hope that inhibitors of individual protein kinases might be tailored to specific diseases based on an understanding of their molecular etiology.[6] Recently, this concept has been dramatically validated by the clinical success of Gleevec, an inhibitor of the Abl tyrosine kinase,[7] in the treatment of chronic mylogenous leukemia, a disease driven by the activity of the BCR-ABL oncogene.

The search for protein kinase inhibitors has led to the realization that not all kinases are equally amenable to targeting with potent, ATP-competitive small molecules. In this regard, a single residue in the ATP binding pocket (corresponding to threonine 338 in Hck) has been shown to control kinase sensitivity to a wide range of structurally unrelated compounds,[1] including pyridinylimidazoles,[8] pyrazolopyrimidines,[2] purines,[9] quinazolines,[10] phenylaminopyrimidines,[11] and staurosporines.[12] This residue is conserved as a threonine or larger amino acid in the human kinome (no wild-type protein kinases contain an alanine or glycine at this position), and structural analysis has shown that the size of this gatekeeper residue restricts access to a pre-existing cavity within the ATP binding pocket.[13] Kinases that possess a threonine at this position are readily targeted by diverse classes of small molecule inhibitors that can access this natural pocket. Moreover, mutation of the gatekeeper residue to a smaller amino acid, such as alanine or glycine, has been shown to induce sensitivity to pyrazolopyrimidine inhibitors at low nanomolar concentrations in over 30 protein kinases—even though in many cases the wild-type kinase is completely insensitive to compounds of this class.[12]

The importance of the gatekeeper in controlling inhibitor sensitivity is underscored by the fact that most kinase inhibitors currently in clinical use target kinases that contain a threonine at this position, even though threonine is found in only ~20% of the human kinome

Keywords: PI3-kinase; Inhibition; Gatekeeper.
* Corresponding author. Tel.: +1 415 514 0472; fax: +1 415 514 0822; e-mail: shokat@cmp.ucsf.edu
† These authors contributed equally to this work.

0968-0896/$ - see front matter © 2005 Elsevier Ltd. All rights reserved.
doi:10.1016/j.bmc.2005.02.021

(e.g., Iressa: EGFR; Gleevec: Abl, PDGFR, and c-Kit; BAY43-9006: Raf). Indeed, analysis of mutations in BCR-Abl that confer drug resistance has shown that mutation of the gatekeeper to a larger amino acid (T315I) is one of the most common mechanisms of resistance to Gleevec.[11] Remarkably, second generation BCR-Abl inhibitors designed to target resistant alleles have been shown to effectively inhibit every naturally occurring mutant of this kinase except those mutated at the gatekeeper residue.[14,15]

Recently, lipid kinases of the phosphoinositide 3-kinase (PI3-K) family have attracted considerable interest as a new class of drug targets.[3,4] These enzymes act by generating the lipid second messengers phosphatidylinositol-3,4-bisphosphate ($PI(3,4)P_2$) and phosphatidylinositol-3,4,5-trisphosphate ($PI(3,4,5)P_3$), which in turn activate downstream enzymes in a wide-range of signaling pathways involved in cell growth, survival, differentiation, and motility.[16] Activating mutations in the PI3-K isoform p110α have recently been identified at high frequency in several types of cancer,[17] and PTEN, the lipid phosphatase that reverses the phosphorylation reaction, has been identified as one of the most commonly inactivated tumor suppressors in the human genome.[18] Moreover, the clinical efficacy of recently approved agents that target the epidermal growth factor receptor in breast[19] and lung[20,21] cancers has been demonstrated to correlate with the dependence of those cancers on aberrant PI3-K signaling and the ability of these agents to suppress that pathway. For these reasons, considerable effort has been directed toward the development of selective inhibitors of these enzymes as potential cancer therapeutics.[22]

Although PI3-Ks possess very low overall sequence homology to protein kinases, they possess the same overall fold, share several consensus sequences (e.g., the DFG motif that is responsible for coordination of Mg^{2+}), and are sensitive to two pan-specific protein kinase inhibitors (staurosporine[23] and quercetin[24]). Due to the importance of these enzymes as an emerging class of drug targets, we sought to identify the residue in lipid kinases analogous to the gatekeeper residue, and to explore how the size of this residue affects the active site structure and inhibitor sensitivity of this class of enzymes.

2. Results and discussion

2.1. The gatekeeper residue is conserved in lipid kinases

The crystal structure of the PI3-K p110γ bound to ATP has been solved,[25] and the catalytic domain was found to share several features with reported protein kinase structures. These similarities include a two-lobed structure consisting of a N-terminal lobe containing a 5–7-stranded β-sheet, a loop connecting two of these strands that interacts with the phosphate groups of ATP, a conserved lysine residue that positions the α and β phosphate groups of ATP for the phosphotransfer reaction, and a primarily α-helical C-terminal lobe that binds the phosphoacceptor. In protein kinases, conserved hydrogen bonds to the N6 and N1 of positions of the adenine ring of ATP are made by the backbone amides of two conserved residues (corresponding to Glu 339 and Met 341 of Hck, respectively). The gatekeeper residue immediately precedes Glu 339, and forms the hydrophobic interior face of the ATP binding pocket, with Cβ of the gatekeeper typically positioned 4–7 Å from the N6 and N7 residues of adenine. Inspection of the ATP binding pocket of p110γ reveals a similar set of contacts. Hydrogen bonds to ATP are made by backbone amides from two residues—Glu 880 and Val 882—and these residues are immediately preceded by a large hydrophobic residue (Ile 879 in p110γ) that is positioned approximately 5 Å from N6 and N7 of adenine (Fig. 1A). To directly compare the orientation of these two residues (Ile 879 in p110γ and Thr 338 in Hck), we superimposed the crystal structures of Hck and p110γ with respect to the adenine ring of ATP using the WebLab Viewer 4.0. This structural alignment indicates that these two residues occupy a largely overlapping, but not identical, space within the interior of the ATP binding pocket, forming the innermost face that contacts the adenine ring of ATP (Fig. 1B). The most important difference between the p110γ and Hck structures in this region is that Cα of Ile 879 in p110γ is shifted slightly perpendicular to the plane of the adenine ring (~2 Å) relative to Thr 338 in Hck, such that Ile 879 also participates in forming the interior roof of the ATP binding pocket, whereas Thr 338 is more completely fixed within the plane of the adenine ring.

To compare this region of primary sequence between PI3-Ks and protein kinases, a structure-based sequence alignment was generated. This analysis reveals that the

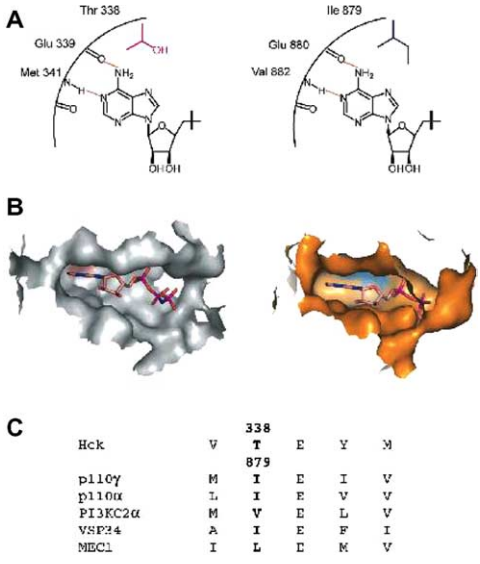

Figure 1. Conservation in the ATP binding pocket of PI3Ks. (A) Schematic illustrating the hydrogen bonding contacts to ATP. (B) Surface representation of the interior face of the ATP binding pocket of Hck (gray) and p110γ (orange), from published crystal structure data. (C) Structure-based sequence analysis of several residues lining the ATP binding pockets of Hck and several PI3Ks.

gatekeeper residue is situated within a small region of sequence homology between lipid and protein kinases (Fig. 1C). As observed for the gatekeeper residue in protein kinases, Ile 879 is conserved as a large hydrophobic residue in all PI3-Ks (isoleucine, leucine, methionine, or valine, although no PI3-Ks contain threonine at this position). The residue immediately following the Ile 879 is conserved in PI3-Ks as a glutamate (83%), and this is also the most common residue at that position in protein kinases (75%). The residues at the −1 and +1/+2 positions relative to Ile 879 in PI3-Ks are conserved as large hydrophobic residues, and the corresponding positions in protein kinases show a similar preference (Fig. 1C). For example, position 337 is either isoleucine, leucine, valine, or methionine in 86% of protein kinases and in 92% of human PI3-Ks. On this basis, we conclude that p110γ residue Ile 879 structurally corresponds to the gatekeeper residue in protein kinases.

As the gatekeeper residue is structurally conserved between PI3-Ks and protein kinases, we asked whether it is also functionally conserved, and in particular whether mutagenesis of this position to a smaller residue might induce inhibitor sensitivity as has been observed for protein kinases.[12] Three representative members of the PI3-K family were selected for this analysis: the yeast PI3-K VPS34, the yeast PI3-K-related protein kinase MEC1, and the prototypical mammalian PI3-K p110α. The gatekeeper residue in each of these kinases was mutated to alanine and glycine, and the effect of this mutation on enzyme activity and inhibitor sensitivity was assessed.

2.2. Effects of gatekeeper mutation on enzymatic activity

Plasmids encoding mutated VPS34 and MEC1 kinases were transformed into *S. cerevisiae* knockout strains, such that the mutant allele functionally replaces the wild-type enzyme. Although yeast are viable in the absence of these proteins, specific growth conditions can induce a requirement for their catalytic activity, allowing us to examine whether the gatekeeper mutated alleles encode active kinases. The activity of VPS34 is required[26] for growth of yeast at elevated temperature (37 °C) or high salt (1.0 M NaCl), whereas MEC1 activity is required[27,28] for growth in the presence of agents that alkylate DNA (0.02% methylmethanesulfonate) or inhibit ribonucleotide reductase (60 mM hydroxylurea). Growth of the mutant strains under these conditions showed that the alanine gatekeeper mutant of VPS34 (I670A) as well as the alanine and glycine gatekeeper mutants of MEC1 (L2129A and L2129G) are able to functionally complement for the knockout at a level comparable to the wild-type enzyme (Fig. 2). Importantly, transformation with the empty vector or a vector containing a catalytically inactive, kinase-dead (kd) mutant of each protein did not to rescue the knockout phenotype, confirming that the observed complementation is due to the catalytic activity of these proteins (Fig. 2).

For p110α, the gatekeeper residue was mutated to alanine and glycine (I848A and I848G) and the mutant kinases were expressed by transient transfection in cos-1 cells. The myc-tagged mutated kinases were purified by immunoprecipitation and their lipid kinase activity was assessed using a kinase assay in vitro. The enzymatic activity of the I848A and I848G mutants was significantly impaired relative to wild-type p110α, with the gatekeeper mutants displaying approximately one-hundredth (I848A) to one-thousandth (I848G) of the wild-type activity (Fig. 3A). The expression level of the wild-type and I848A proteins was similar by western blotting (Fig. 3B), suggesting that the gatekeeper mutation had disrupted the integrity of the enzyme active site in this mutant without globally destabilizing the protein.

As VPS34 and MEC1 appear to tolerate the gatekeeper mutation, the impaired activity of I848A p110α was surprising, and led us to search for differences in primary sequence between these related kinases that might account for the observed differences in biochemical activity. Based on the crystal structure of p110γ, the

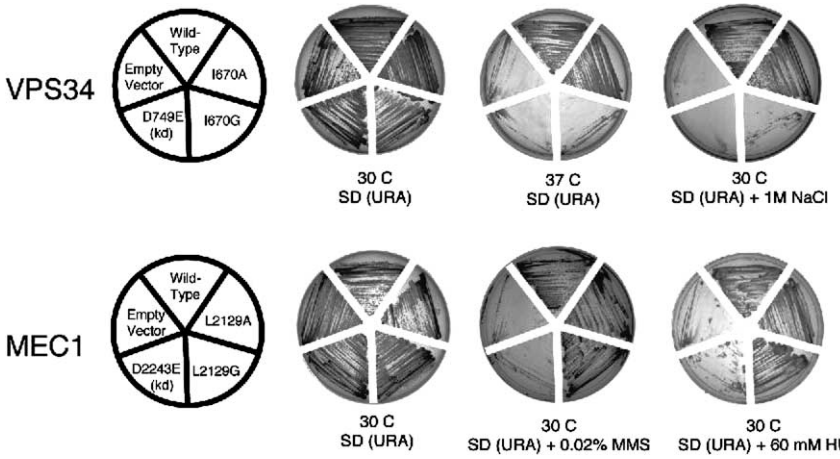

Figure 2. Growth of yeast expressing various alleles of VPS34 and MEC1 under nonselective and selective growth conditions. *S. cerevisiae* expressing VPS34 alleles (wild type, empty vector, kinase dead (kd; D749E), I670G, or I670A) were plated on nonselective media (SD(URA)) or selective media (SD(URA), 1 M NaCl). *S. cerevisiae* expressing MEC1 alleles (wild type, empty vector, kinase dead (kd; D2243E), L2129G, or L2129A) were plated on media (SD(URA)) or selective media (SD(URA), 0.02% (MMS); or SD(URA), 60 mM hydroxyurea (HU)).

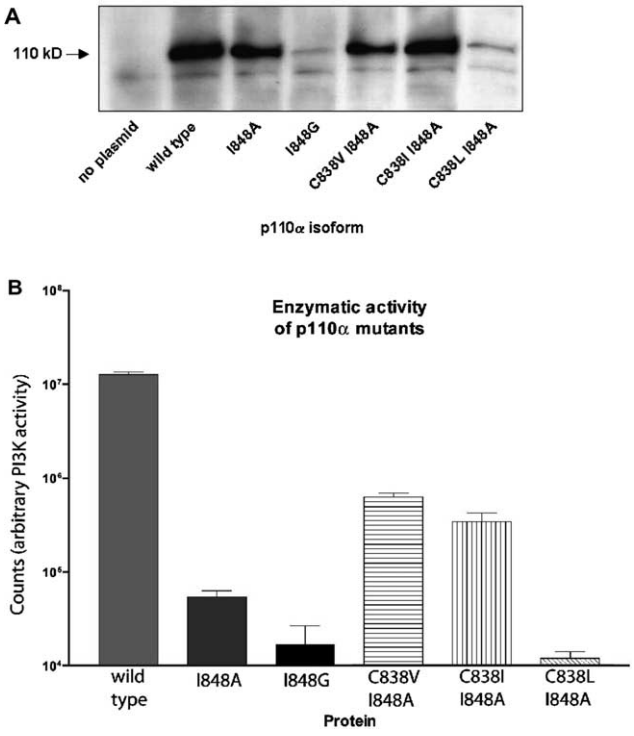

Figure 3. Relative expression levels and enzymatic activities of Myc-tagged p110α alleles. (A) Equal amounts of soluble protein (29 μg) from transiently transfected cos-1 cells were subjected to Western analysis (anti-Myc antibody, 9E10). (B) Relative enzymatic activities of p110α alleles. Cos-1 cells were co-transfected with equal amounts of expression vectors containing the indicated genes and p85 (a p110α adaptor protein). Protein was immunoprecipitated (anti-Myc antibody) from 950 μg of total soluble protein, and the activity assay was performed. Error bars represent the standard deviation from the mean from three independent measurements.

residues that form the core of the ATP binding pocket were identified, and these residues were aligned among 15 members of the PI3-K family (Fig. 4). We then identified residues that are common to VPS34 and MEC1, but different in p110α, that might account for the observed difference in tolerating the gatekeeper mutation. This analysis focused our attention on cysteine 838 in p110α (Position 13, Fig. 4). Among the class I PI3-Ks such as p110α, this residue is conserved as a cysteine, whereas among the class III PI3Ks (e.g., VPS34) and PI3-K-related protein kinases (e.g., MEC1), this residue is conserved as a β-branched residue (valine or isoleucine). Importantly, inspection of the crystal structure of p110γ reveals that C838 is located in β-strand 6, directly adjacent to I848 in β-strand 7 (Fig. 5), suggesting that it may cooperate with the gatekeeper residue to stabilize this region of the protein. As β-branched amino acids have been shown to promote β-sheet formation,[29] we reasoned that the presence of an isoleucine or valine residue at this position might stabilize that region of the protein when the gatekeeper is mutated, and thereby account for the differences in activity between MEC1/VPS34 and p110α.

To test this hypothesis, we prepared double mutants of p110α containing the I848A gatekeeper mutation in the context of second site mutations C838V, C838I, and C838L. The double mutant enzymes were expressed in cos-1 cells, and their expression levels and enzymatic activity was assessed. The I848A/C838V and I848A/C838I double mutants both showed ~10-fold increased enzymatic activity relative to the I848A single mutant enzyme (Fig. 3A). This enhancement in activity occurred without significantly changing the expression level of the protein (Fig. 3B), and confirms that mutation of this position to a β-branched residue can restore enzymatic activity in the background of the gatekeeper mutation. Strikingly, the I848A/C838L double mutant enzyme showed virtually undetectable catalytic activity and expression of this protein could not be detected by western blotting (Fig. 3), indicating that the isomeric I848A/C838I and I848A/C838L p110α proteins have dramatically different stability. This suggests that the enhanced activity of the isoleucine and valine mutants is likely a specific consequence of the β-branched residue at position 838 stabilizing β-strands 6 and 7, rather than a nonspecific consequence of additional hydrophobic surface in the protein core.

2.3. Effects of gatekeeper mutation on inhibitor sensitivity

We next sought to assess how mutation of the gatekeeper residue to a smaller amino acid would affect inhibitor sensitivity. In protein kinases, mutation of the gatekeeper to alanine or glycine has been shown to induce sensitivity to both pyrazolopyrimidine inhibitors based on the Src-family kinase inhibitor PP1 and analogs of the natural product K252a.[12] p110γ has been shown to be sensitive to staurosporine (K_d = 0.29 μM),[23] which is structurally related to K252a, suggesting that K252a analogs may also target engineered lipid kinases. Although wild-type PI3-Ks are not sensitive to the protein kinase inhibitor PP1, mutation of the gatekeeper residue in protein kinases can induce sensitivity to this class of compounds in kinases that otherwise show no affinity for this scaffold.[12] Following this reasoning, we screened a small panel of these compounds in vitro against the wild-type and I848A p110α and in vivo against the wild-type and I670A mutant VPS34 (Supplementary Fig. 1). None of these compounds showed selective inhibition of the I848A allele of p110α at a concentration of 50 μM in vitro or I670A VPS34 at a concentration of 1 mM in a yeast halo assay. These results suggest that the structural differences between protein and lipid kinases may be too significant to bridge with a single inhibitor scaffold, and that new inhibitor analogs may be necessary to explore the gatekeeper pocket in lipid kinases.

To probe more directly the engineered gatekeeper pocket, we prepared a panel of analogs of the PI3-K inhibitor LY294002.[30] LY294002 reversibly inhibits PI3-Ks at IC_{50} values in the low micromolar range, but shows little selectivity among individual family members.[31] The crystal structure of LY294002 bound to p110γ has been solved,[23] and reveals that the C3 position of LY294002 is located adjacent to the gatekeeper residue at a distance of approximately 4 Å. Molecular modeling based on this structure suggests that analogs of LY294002

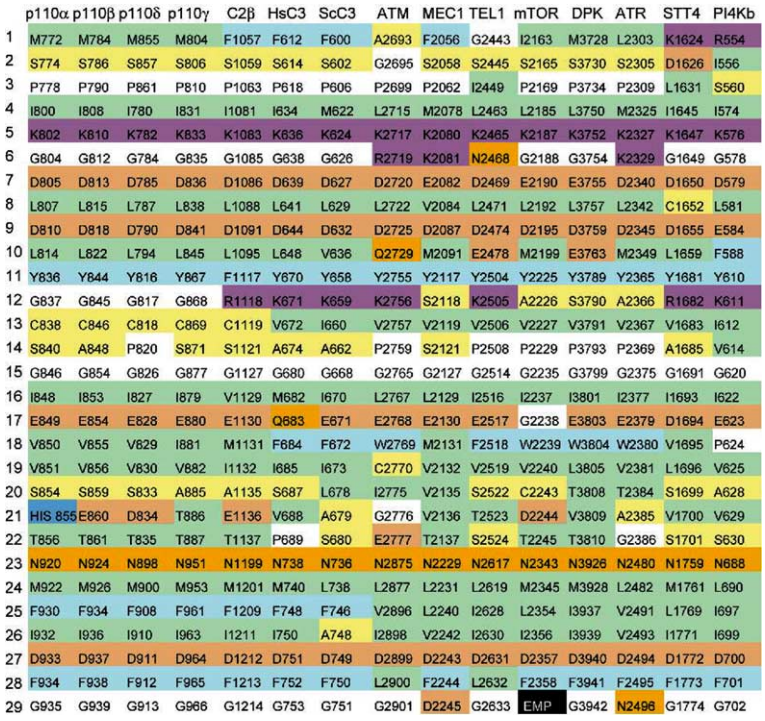

	p110α	p110β	p110δ	p110γ	C2β	HsC3	ScC3	ATM	MEC1	TEL1	mTOR	DPK	ATR	STT4	PI4Kb
1	M772	M784	M855	M804	F1057	F612	F600	A2693	F2056	G2443	I2163	M3728	L2303	K1624	R554
2	S774	S786	S857	S806	S1059	S614	S602	G2695	S2058	S2445	S2165	S3730	S2305	D1626	I556
3	P778	P790	P861	P810	P1063	P618	P606	P2699	P2062	I2449	P2169	P3734	P2309	L1631	S560
4	I800	I808	I780	I831	I1081	I634	M622	L2715	M2078	L2463	L2185	L3750	M2325	I1645	I574
5	K802	K810	K782	K833	K1083	K636	K624	K2717	K2080	K2465	K2187	K3752	K2327	K1647	K576
6	G804	G812	G784	G835	G1085	G638	G626	R2719	K2081	N2468	G2188	G3754	K2329	G1649	G578
7	D805	D813	D785	D836	D1086	D639	D627	D2720	E2082	D2469	E2190	E3755	D2340	D1650	D579
8	L807	L815	L787	L838	L1088	L641	L629	L2722	V2084	L2471	L2192	L3757	L2342	C1652	L581
9	D810	D818	D790	D841	D1091	D644	D632	D2725	D2087	D2474	D2195	D3759	D2345	D1655	E584
10	L814	L822	L794	L845	L1095	L648	V636	Q2729	M2091	E2478	M2199	E3763	M2349	L1659	F588
11	Y836	Y844	Y816	Y867	F1117	Y670	Y658	Y2755	Y2117	Y2504	Y2225	Y3789	Y2365	Y1681	Y610
12	G837	G845	G817	G868	R1118	K671	K659	K2756	S2118	K2505	A2226	S3790	A2366	R1682	K611
13	C838	C846	C818	C869	C1119	V672	I660	V2757	V2119	V2506	V2227	V3791	V2367	V1683	I612
14	S840	A848	P820	S871	S1121	A674	A662	P2759	S2121	P2508	P2229	P3793	P2369	A1685	V614
15	G846	G854	G826	G877	G1127	G680	G668	G2765	G2127	G2514	G2235	G3799	G2375	G1691	G620
16	I848	I853	I827	I879	V1129	M682	I670	L2767	L2129	I2516	I2237	I3801	I2377	I1693	I622
17	E849	E854	E828	E880	E1130	Q683	E671	E2768	E2130	E2517	G2238	E3803	E2379	D1694	E623
18	V850	V855	V829	I881	M1131	F684	F672	W2769	M2131	F2518	W2239	W3804	W2380	V1695	P624
19	V851	V856	V830	V882	I1132	I685	I673	C2770	V2132	V2519	V2240	L3805	V2381	L1696	V625
20	S854	S859	S833	A885	A1135	S687	L678	I2775	V2135	S2522	C2243	T3808	T2384	S1699	A628
21	HIS 855	E860	D834	T886	E1136	V688	A679	G2776	V2136	T2523	D2244	V3809	A2385	V1700	V629
22	T856	T861	T835	T887	T1137	P689	S680	E2777	T2137	S2524	T2245	T3810	G2386	S1701	S630
23	N920	N924	N898	N951	N1199	N738	N736	N2875	N2229	N2617	N2343	N3926	N2480	N1759	N688
24	M922	M926	M900	M953	M1201	M740	L738	L2877	L2231	L2619	M2345	M3928	L2482	M1761	L690
25	F930	F934	F908	F961	F1209	F748	F746	V2896	L2240	I2628	L2354	I3937	V2491	L1769	I697
26	I932	I936	I910	I963	I1211	I750	A748	I2898	V2242	I2630	I2356	I3939	V2493	I1771	I699
27	D933	D937	D911	D964	D1212	D751	D749	D2899	D2243	D2631	D2357	D3940	D2494	D1772	D700
28	F934	F938	F912	F965	F1213	F752	F750	L2900	F2244	L2632	F2358	F3941	F2495	F1773	F701
29	G935	G939	G913	G966	G1214	G753	G751	G2901	D2245	G2633	EMP	G3942	N2498	G1774	G702

Figure 4. Structure-based sequence alignment of 15 members of the PI3K family. Residue coloring: hydrophobic aliphatic (green), hydrophobic aromatic (light blue), small (yellow), polar charged (dark blue), basic (purple), and acidic (orange).

containing extended substituents at C3 would access the nascent pocket created by the gatekeeper mutation (Fig. 5). A series of C3-substituted analogs of LY294002 were designed (lacking the 8-phenyl group of LY294002, as this moiety has been shown to be dispensable for binding to PI3-Ks[30]) and a panel of such analogs was prepared. This series of compounds was designed to include analogs that possess C3 substituents similar in size to the space created directly by the isoleucine to alanine mutation (e.g., Et, *n*-Pr), as well as those that contain much larger substituents (Ph, Bn). These latter compounds were included to probe whether the gatekeeper mutation would allow access to a deeper cavity within the kinase active site; in protein kinases, mutation of the gatekeeper has been shown to facilitate binding of substrate and inhibitor analogs containing bulky substituents much larger than the space created directly by the amino acid change.[12,13]

Synthesis was accomplished by addition of an excess of the appropriate Grignard reagent to salicylaldehyde to afford benzylic alcohols **1c**–**g** (Scheme 1). The resulting alcohols were oxidized to the corresponding ketones **2c**–**g** using MnO_2, and the ring closing was performed using a morpholine phosgeniminium salt[30,34] to afford the desired 3-substituted analogs of LY294002 in high purity as white solids.

This panel of LY294002 analogs was tested for inhibition of the wild-type and C838V/I848A mutant of p110α in a PI3-K assay in vitro (Table 1). Both LY294002 and the desphenyl analog LY292223 inhibited wild-type and C838V/I848A p110α at low micromolar concentrations, although inhibition by LY292223 was modestly reduced for the double mutant. As the size of the C3-moiety was increased, IC_{50} values against both the mutant and wild-type p110α increased by ~10 to >100-fold, and this increase tracked with the size of the C3 substituent, with the weakest inhibition by compounds **3g** (Ph) and **3h** (Bn). Surprisingly, only compound **3c** (Et) showed enhanced binding to mutant p110α relative to wild-type p110α, with modest selectivity for the engineered kinase (~6-fold). This compound contains an ethyl moiety at the C3 position, which is the most similar in size to the space created directly by the amino acid change (Ile to Ala) at the gatekeeper position. This suggests that mutation of this residue does create a corresponding cavity in the kinase active site, but that this cavity does not expose a preexisting pocket or allow for the binding of significantly larger inhibitor analogs with enhanced affinity, as has been observed in the protein kinase family.

3. Conclusions

We have explored the role of the gatekeeper residue in PI3-Ks by a convergent engineering approach that combines mutagenesis of the target residue with design of inhibitor analogs to complement this mutation. This study suggests that mutation of the gatekeeper residue in lipid kinases can create a nonnatural pocket, but that this mutation does not provide access to a deeper pocket such as that found in protein kinases. This difference may reflect the different way that protein and lipid kinases utilize their primary sequence to construct the innermost wall of the ATP binding pocket. Crystal structures of protein kinases reveal that residues from

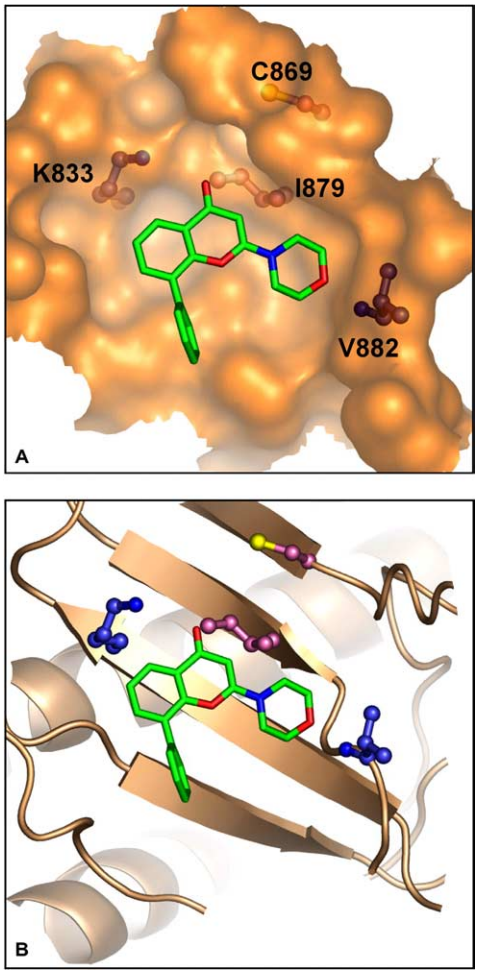

Figure 5. Co-crystal structure of p110γ-LY294002. (A) Surface representation and (B) ribbon representation of the protein illustrating the important hydrogen-bonding contacts and residues mutated in this study.

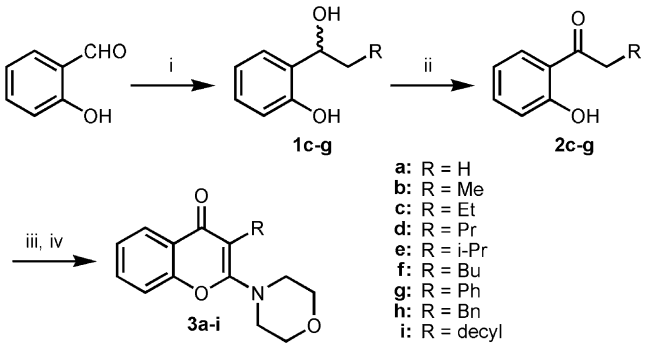

Scheme 1. Reagents and conditions: (i) Grignard reagent, THF; (ii) MnO_2, CH_2Cl_2; (iii) $TiCl_4$, *i*-Pr_2EtN, CH_2Cl_2; (iv) 4-dichloromethylenemorpholin-4-ium chloride.

β-strand 5, which include the gatekeeper, form the deepest face of the ATP binding pocket, and that most of the contacts that this face makes with adenine involve the side chain of the gatekeeper residue directly. By comparison, in the crystal structure of p110γ, the gatekeeper is shifted upward and away from the N6 of adenine by ~2 Å. To help fill this space, the side chain of Tyr 867 from β-strand 6 (which is otherwise positioned in a second sphere of residues that do not contact ATP directly) infiltrates the ATP binding pocket to make a direct contact with adenine near N6. The analogous residue in protein kinases (corresponding to Leu 325 in Hck) is positioned within a second sphere that is obstructed from accessing ATP by the gatekeeper. Thus, it appears that in lipid kinases two residues (Tyr 867 and Ile 879) collaborate to fill the space that is otherwise occupied by a single residue in protein kinases. Unfortunately, we have found that mutation of Tyr 836 in p110α (which corresponds to Tyr 867 in p110γ) to any other amino acid tested (glycine, alanine, threonine, aspartic acid, leucine, methionine, or histidine) results in a complete loss of catalytic activity, indicating that this region of the protein is not amenable to structural modification (Z.A.K. and K.M.S., unpublished observations). These results, as well as the nearly perfect conservation of Tyr 867 within the PI3-K family (Fig. 4), suggest that a different set of residues in lipid kinases are likely responsible for controlling sensitivity to small molecule inhibitors. Ultimately, the identification of rules guiding inhibitor sensitivity for this important family of enzymes will require the discovery of new structural classes of PI3-K inhibitors and the broad characterization of their specificity against individual PI3-K isoforms, a process that is currently underway in our laboratory[31] and others.[32]

Table 1. IC_{50} values of LY292223 analogues against wild type and mutant p110α enzymes

Analogue	IC_{50} (μM)	
	Wild type	C838V I848A
LY294002	1.1	1.1
LY292223 (**3a**)	2.6	15
3b (Me)	33	40
3c (Et)	28	4.4
3d (Pr)	31	68
3e (*i*-Pr)	51	>200
3f (Bu)	25	48
3g (Ph)	>200	>200
3h (Bn)	>200	>200

4. Experimental

4.1. Protein expression

Mutations were introduced by Quikchange (Stratagene), and confirmed using standard dideoxy-based sequencing. Myc-tagged p110α was expressed by transient transfection of cos-1 cells. Cells were lysed in lysis buffer (50 mM Tris (pH 7.4), 300 mM NaCl, 5 mM EDTA, 0.02% NaN_3, 1% Triton X-100), protease inhibitors (protease inhibitor cocktail tablets (Roche); sodium orthovanadate (8 mM); PMSF (83 μM)), and 8 mM DTT. The kinase was immunoprecipitated using a Protein-G-9E10 antibody complex, and washed twice with buffer A (PBS, 1 mM EDTA, 1% Triton X-100), twice with buffer B (100 mM Tris (pH 7.4), 500 mM LiCl, 1 mM EDTA), twice with buffer C (50 mM Tris (pH 7.4), 100 mM NaCl), and once with PBS. In control

experiments, no differences in inhibitor sensitivity were observed between wild type p110α protein that was obtained from transfected cos-1 cells, Sf9 cells using a baculovirus system, or commercially available recombinant protein (Jena Bioscience).

For SDS-PAGE and Western blot analyses, protein concentrations in cell lysates were determined using a Bradford assay. Proteins were loaded onto a Tris-glycine gel (8–16% gradient; Gradipore) and separated by SDS-PAGE before being transferred onto a nitrocellulose membrane. The blot was treated with blocking reagent (5% dry milk in TBST) for 1 h, then primary antibody (9E10 (anti-Myc; Santa Cruz Biotech), 1:500 in TBST) overnight at 4 °C. The blot was then rinsed (5 min each) with deionized water (1 × 20 mL) and TBST (3 × 20 mL) before treatment with secondary anti-mouse-HRP antibody (1:1000 in TBST) for 30 min at rt.

4.2. PI3-Kinase enzymatic assay

The PI3-K assay was performed essentially as described.[31] Briefly, a mixture of kinase, inhibitor, buffer (25 mM HEPES (pH 7.4), 10 mM $MgCl_2$), and freshly sonicated phosphatidylinositol (200 μg/mL) was prepared at 4 °C, and aliquotted into eppendorf tubes. The tubes were allowed to warm to rt over 5 min, and the enzymatic reaction was initiated with the addition of ATP (10 μCi γ-^{32}P-ATP; final [ATP] = 20 nM). Reactions were incubated for 20 min at rt, and quenched by addition of 1 M HCl (105 μL) followed by 1:1 MeOH–$CHCl_3$ (160 μL). The resulting biphasic mixture was vortexed (ca. 5 s), briefly centrifuged (ca. 5 s), and the organic phase (~100 μL) was transferred to a new tube using a gel-loading tip pre-coated with $CHCl_3$. This extract was spotted on TCL plates (silica gel 60 F254, 250 μm) and developed for 3–4 h using 65:35 1-propanol–2 M AcOH as eluent. The TLC plates were then air-dried (ca. 45 min), and the reaction products quantitated using a phosphorimager (Molecular Dynamics). For each compound, kinase activity was measured at 15 inhibitor concentrations representing twofold dilutions from the highest concentration tested (usually 400 μM). For compounds showing significant activity, IC_{50} value determinations were repeated (2–5 times) and the value reported is the average of these independent measurements. Preincubation of the enzyme with cold ATP (1 μM, 10 min) was sometimes used to suppress the observation of radiolabeled impurities that were kinase-independent (data not shown). In control experiments, no difference was observed in inhibitor sensitivity between performing the assay in the absence or presence (1 μM) of cold ATP.

4.3. Analysis of yeast expressing PI3-K mutant alleles

The VPS34 *S. cerevisiae* knockout strain 15149 was obtained from the ATCC. The MEC1/SML1 *S. cerevisiae* knockout strain yBRT7-4b was a gift from David Toczyski (UCSF). Knockout strains were transformed with plasmids (pRS416 CEN URA3) encoding wild-type and mutant VPS34 and MEC1 and transformants were selected on SD-URA media. Cells were streaked onto plates containing SD-URA or the same media supplemented with either 1 M NaCl (VPS34) or 0.02% MMS or 60 mM HU (MEC1), grown at 30 or 37 °C for 3 days, and photographed.

4.4. Chemical synthesis

4.4.1. General methods. All reactions were performed under argon in oven- or flame-dried glassware fitted with rubber septa, and were stirred magnetically. Thin layer chromatography was performed on Merck precoated silica gel F-254 plates (0.25 mm). Flash column chromatography was performed using Merck silica gel 60 (230–400 mesh). Proton NMR spectra were recorded at 400 MHz and are reported in δ (ppm) as s (singlet), d (doublet), t (triplet), q (quartet), m (multiplet), or br (broad), and are referenced to the residual solvent signal: $CDCl_3$ (7.26) or C_6D_6 (7.15). Carbon NMR spectra were recorded at 100 MHz and are reported in δ (ppm), and are referenced to the solvent signal: $CDCl_3$ (77.0), C_6D_6 (128.0). Infrared spectra were recorded on a Nicolet Impact 400 spectrometer using thin films of sample and resonances are reported in wavenumbers (cm^{-1}). Mass spectra were recorded on a VG-70S mass spectrometer and are reported in units of mass/charge (*m*/*z*). Unless otherwise noted, all materials were obtained from commercial sources and used without further purification. In experiments involving air- or moisture-sensitive compounds, solvents and reagents were either distilled or purchased as anhydrous grade material. Dichloromethylenemorpholin-4-ium chloride was prepared according to literature procedures.[33,34]

4.4.2. General procedure for the preparation of alcohols 1c–g. A round bottom flask charged with salicylaldehyde and THF was cooled to −78 °C. To this mixture was added the appropriate Grignard reagent (5–10 equiv) by syringe over 10 min, and the resulting mixture was allowed to stir at −78 °C for 10 min. The stirred reaction mixture was allowed to warm to rt overnight. In air, this mixture was slowly added to a 0 °C saturated NH_4Cl solution. The aqueous phase was extracted with ether and the combined organic phases were dried over Na_2SO_4, filtered, and concentrated to give a crude oil. Further purification and characterization of each derivative is described below.

4.4.2.1. 2-(1-Hydroxybutyl)phenol (1c). Synthesis was performed using the general procedure described above using 1.15 g salicylaldehyde (9.4 mmol), 94 mL THF, 94 mmol propylmagnesium chloride (47 mL of 2.0 M solution in ether), saturated NH_4Cl solution (75 mL), and ether (3 × 40 mL). The crude oil was purified by flash column chromatography (SiO_2, 10% EtOAc–hexanes) to give a clear, pale yellow oil (1.226 g, 7.4 mmol, 79%). ^{1}H NMR: ($CDCl_3$) δ 8.16 (s, 1H), 7.12 (t, *J* = 8 Hz, 1H), 6.91 (d, *J* = 8 Hz, 1H), 6.82 (m, 2H), 4.76 (t, *J* = 7 Hz, 1H), 3.35 (s, 1H), 1.83 (m, 1H), 1.74 (m, 1H), 1.43 (m, 1H), 1.30 (m, 1H), 0.91 (t, *J* = 8 Hz, 3H). ^{13}C{^{1}H} NMR: ($CDCl_3$) δ 155.2, 128.7, 127.8, 127.2, 119.7, 116.9, 75.5, 39.3, 18.9, 13.8. IR: 3321. HRMS: (EI) calcd for $C_{10}H_{14}O_2$ (M^+) 166.0994; found

166.0995. Anal. Calcd for $C_{10}H_{14}O_2$: C, 72.26; H, 8.49. Found: C, 72.19; H, 8.41.

4.4.2.2. 2-(1-Hydroxypentyl)phenol (1d).[35,36] Synthesis was performed using the general procedure described above using 2.29 g salicylaldehyde, 100 mL THF, 94 mmol of butylmagnesium chloride (47 mL of 2.0 M solution in THF), saturated NH_4Cl solution (75 mL), and ether (4 × 50 mL). The crude oil was purified by flash column chromatography (SiO_2, 10% EtOAc–hexanes) to give a clear colorless oil (3.37 g, 18.7 mmol, 99%). ^{1}H NMR: ($CDCl_3$) δ 8.32 (s, 1H), 7.12 (m, 1H), 6.93 (m, 1H), 6.82 (m, 2H), 4.74 (t, J = 7 Hz, 1H), 3.84 (br s, 1H), 1.90–1.71 (m, 2H), 1.44–1.22 (m, 4H), 0.90 (t, J = 7 Hz, 3H). Lit.[35] δ 7.93 (s, 1H), 7.4–6.7 (m, 4H), 4.82 (t, J = 5.6 Hz, 1H), 2.53 (br, 1H), 2.0–1.1 (m, 6H), 0.90 (t, J = 5.9 Hz, 3H). ^{13}C{^{1}H} NMR: ($CDCl_3$) δ 155.2, 128.7, 128.2, 127.0, 119.8, 117.0, 73.8, 46.0, 24.5, 23.1, 22.0. IR: 3357. HRMS: (EI) 180.1150 calcd for $C_{11}H_{16}O_2$ (M^+); found 180.1144. Lit.[35] 180.1150 calcd for $C_{11}H_{16}O_2$ (M^+); found 180.1119.

4.4.2.3. 2-(1-Hydroxy-3-methylbutyl)phenol (1e). Synthesis was performed using the general procedure described above using 1.15 g salicylaldehyde, 95 mL THF, 94 mmol of isobutylmagnesium bromide (47 mL of 2.0 M solution), saturated NH_4Cl (75 mL), and ether (3 × 50 mL). The crude oil was purified by flash column chromatography (SiO_2, 10% EtOAc–hexanes) to give a clear, pale yellow oil (1.66 g, 9.2 mmol, 98%). ^{1}H NMR: ($CDCl_3$) δ 8.09 (s, 1H), 7.12 (m, 1H), 6.91 (m, 1H), 6.81 (m, 2H), 4.84 (br d, J = 3 Hz, 1H), 3.22 (s, 1H), 1.81 (m, 1H), 1.70 (m, 1H), 1.56 (m, 1H), 0.93 (m, 6H). Lit.[38] (CCl_4–C_6D_6 7:1) δ 7.76 (s, 1H), 6.50–7.20 (m, 4H), 4.50–4.90 (m, 1H), 2.55 (s, 1H), 1.00–2.00 (m 3H), 0.75–1.00 (m, 6H). ^{13}C{^{1}H} NMR: ($CDCl_3$) δ 155.2, 128.6, 128.1, 126.9, 119.8, 116.9, 73.7, 45.9, 24.5, 23.0, 22.0. IR: 3341. Lit.[38] 3384 (s, b), 1596 (m), 1384 (m), 1372 (m), 760 (s). HRMS: (EI) 180.1150 calcd for $C_{11}H_{16}O_2$ (M^+); found 180.1152.

4.4.2.4. 2-(1-Hydroxyhexyl)phenol (1f). Synthesis was performed using the general procedure described above using 2.29 g salicylaldehyde, 100 mL THF, 80 mmol of pentylmagnesium bromide (40 mL of 2.0 M solution), saturated NH_4Cl (75 mL), and ether (3 × 50 mL). The crude oil was purified by flash column chromatography (SiO_2, 10% EtOAc–hexanes) to give a clear, pale yellow oil (3.6 g, 18.7 mmol, 99%). ^{1}H NMR: ($CDCl_3$) δ 8.44 (s, 1H), 7.12 (m, 1H), 6.96 (m, 1H), 6.83 (m, 2H), 4.76 (br m, 1H), 4.16 (br s, 1H), 1.91–1.72 (m, 2H), 1.48–1.38 (m, 1H), 1.30 (m, 5H), 0.91 (t, J = 7 Hz, 3H). ^{13}C{^{1}H} NMR: ($CDCl_3$) δ 155.5, 128.5, 127.9, 127.1, 119.9, 116.8, 75.5, 37.1, 31.5, 25.3, 22.5, 13.9. IR: 3348. HRMS: (EI) 194.1306 calcd for $C_{12}H_{18}O_2$ (M^+); found 194.1302. Combustion analysis was not obtained for this compound due to its similarity to **1c**–**g**.

4.4.2.5. 2-(1-Hydroxy-2-phenylethyl)phenol (1g). Synthesis was performed using the general procedure described above using 1.15 g salicylaldehyde, 95 mL THF, 94 mmol of benzylmagnesium bromide (47 mL of 2.0 M solution in THF), saturated NH_4Cl (75 mL), and ether (3 × 50 mL). The crude oil was purified by flash column chromatography (SiO_2, 50% EtOAc–hexanes) to give a colorless solid (1.42 g, 6.6 mmol, 75%). ^{1}H NMR: ($CDCl_3$) δ 8.01 (s, 1H), 7.34–7.14 (m, 5H), 6.93–6.79 (m, 4H), 4.98 (dt, J = 3 Hz, J = 7 Hz, 1H), 3.10 (d, J = 7 Hz, 2H), 2.81 (d, J = 3 Hz, 1H). Lit.[37] (partial) δ 5.02 (t, J = 7 Hz, 1H), 3.11 (d, J = 7 Hz, 2H). ^{13}C{^{1}H} NMR: ($CDCl_3$) δ 151.6, 133.6, 125.8, 125.3, 125.0, 123.5, 123.3, 122.8, 116.1, 113.5, 73.0, 40.4. IR: 3327. HRMS: (EI) 214.0993 calcd for $C_{14}H_{14}O_2$ (M^+); found 214.1003.

4.4.3. General procedure for the preparation of ketones 2c–g. A round bottom flask was charged with the appropriate diol **1**, MnO_2, and CH_2Cl_2, and stirred for 7 h at rt. The heterogeneous reaction mixture was filtered through a pad of Celite, and the solids were washed with 500 mL CH_2Cl_2. The filtrate was concentrated in vacuo to give a crude oil. The crude oil was purified by flash column chromatography (SiO_2, 10% EtOAc–hexanes) to give a colorless oil. Characterization of each derivative is described below.

4.4.3.1. 1-(2-Hydroxyphenyl)butan-1-one (2c). Synthesis was performed using the general procedure described above using **1c** (2.5 g, 15.1 mmol), MnO_2 (11.5 g, 132 mmol), and CH_2Cl_2 (140 mL). Compound **2c** was isolated as a colorless oil (1.13 g, 6.9 mmol, 46%). ^{1}H NMR: ($CDCl_3$) δ 12.38 (s, 1H), 7.68 (dd, J = 1 Hz, J = 7 Hz, 1H), 7.36 (dt, J = 2 Hz, J = 7 Hz, 1H), 6.90 (dd, J = 1 Hz, J = 7 Hz, 1H), 6.80 (dt, J = 2 Hz, J = 7 Hz, 1H), 2.87 (t, dt, J = 8 Hz, 2H), 1.70 (sextet, J = 8 Hz, 2H), 0.96 (t, J = 8 Hz, 3H). Lit.[40] δ 12.40 (s, 1H), 7.82–6.80 (m, 4H), 2.96 (t, J = 7.4 Hz, 2H), 1.78 (sextet, J = 7.4 Hz, 2H), 1.02 (t, J = 7.4 Hz, 3H). ^{13}C{^{1}H} NMR: ($CDCl_3$) δ 206.7, 162.5, 136.1, 129.9, 119.3, 118.8, 118.4, 40.1, 17.8, 13.7. Lit.[40] δ 206.79, 162.49, 136.17, 130.00, 119.36, 118.82, 118.48, 40.17, 17.90, 13.38. IR: 1641, 1614, 1581, 1488, 1447, 1265, 1202, 1158, 754. Lit.[40] 1640, 1448, 1226, 1203. HRMS: (EI) 164.0837 calcd for $C_{10}H_{12}O_2$ (M^+); found 164.0840. Lit.[40] 164. Anal. Calcd for $C_{10}H_{12}O_2$: C, 73.15; H, 7.37. Found: C, 73.22; H, 7.45.

4.4.3.2. 1-(2-Hydroxyphenyl)pentan-1-one (2d).[36] Synthesis was performed using the general procedure described above using **1d** (2.0 g, 11.1 mmol), MnO_2 (9.7 g, 110 mmol), and CH_2Cl_2 (100 mL). Compound **2d** was isolated as a colorless oil (796 mg, 4.47 mmol, 40%). ^{1}H NMR: ($CDCl_3$) δ 12.38 (s, 1H), 7.71 (dd, J = 1 Hz, J = 8 Hz, 1H), 7.41 (m, 1H), 6.92 (dd, J = 1 Hz, J = 8 Hz, 1H), 6.84 (m, 1H), 2.93 (t, J = 7 Hz, 2H), 1.68 (m, 2H), 1.38 (m, 2H), 0.93 (t, J = 7 Hz, 3H). ^{13}C{^{1}H} NMR: ($CDCl_3$) δ 208.7, 162.3, 135.9, 129.8, 119.0, 118.5, 118.2, 37.8, 26.3, 22.1, 13.6. IR: 1640, 1582, 1487, 1446, 1353, 1249, 119, 1157, 753. HRMS: (EI) 178.0994 calcd for $C_{11}H_{14}O_2$ (M^+); found 178.0996. Combustion analysis was not obtained for this compound due to its similarity to **2c**–**g**.

4.4.3.3. 1-(2-Hydroxyphenyl)-3-methylbutan-1-one (2e). Synthesis was performed using the general proce-

dure described above using **1e** (2.0 g, 11.1 mmol), MnO_2 (10.0 g, 115 mmol), and CH_2Cl_2 (120 mL). Compound **2e** was isolated as a colorless oil (650 mg, 3.65 mmol, 33%). ^1H NMR: ($CDCl_3$) δ 12.45 (s, 1H), 7.69 (dd, $J = 2$ Hz, $J = 8$ Hz, 1H), 7.38 (dt, $J = 2$ Hz, $J = 8$ Hz, 1H), 6.91 (dd, $J = 2$ Hz, $J = 8$ Hz, 1H), 6.82 (dt, $J = 2$ Hz, $J = 8$ Hz, 1H), 2.77 (d, $J = 7$ Hz, 2H), 2.24 (nonet, $J = 6$ Hz, 1H), 0.96 (d, $J = 6$ Hz, 6H). Lit.[40] δ 12.47 (s, 1H), 7.81–6.82 (m, 4H), 2.85 (d, $J = 6.9$ Hz, 2H), 1.78 (nonet, $J = 6.7$ Hz, 1H), 1.02 (d, $J = 6.6$ Hz, 6H). $^{13}C\{^1H\}$ NMR: ($CDCl_3$) δ 206.4, 162.5, 136.0, 130.0, 119.5, 118.6, 118.3, 46.9, 25.3, 22.5. Lit.[40] δ 207.2, 163.1, 136.7, 130.6, 120.1, 119.3, 119.0, 47.6, 26.0, 23.2. IR: 1638, 1488, 1447, 1306, 1202, 1158, 753. Lit.[40] 1639, 1488, 1447, 1158. HRMS: (EI) 178.0994 calcd for $C_{11}H_{14}O_2$ (M^+); found 178.0999. Lit.[40] 178.

4.4.3.4. 1-(2-Hydroxyphenyl)hexan-1-one (2f). Synthesis was performed using the general procedure described above using **1f** (2.0 g, 10.3 mmol), MnO_2 (8.0 g, 92 mmol), and CH_2Cl_2 (110 mL). Compound **2f** was isolated as a colorless oil (900 mg, 4.68 mmol, 46%). ^1H NMR: ($CDCl_3$) δ 12.38 (s, 1H), 7.70 (dd, $J = 2$ Hz, $J = 8$ Hz, 1H), 7.40 (m, 1H), 6.92 (m, 1H), 6.83 (m, 1H), 2.92 (t, $J = 7$ Hz, 2H), 1.70 (m, 2H), 1.33 (m, 4H), 0.88 (t, $J = 7$ Hz, 3H). Lit.[40] δ 12.40 (s, 1H), 7.82–6.80 (m, 4H), 2.98 (t, $J = 7.6$ Hz, 2H), 1.84–1.25 (m, 6H), 0.91 (t, $J = 6.7$ Hz, 3H). $^{13}C\{^1H\}$ NMR: ($CDCl_3$) δ 206.8, 162.4, 136.0, 129.9, 119.2, 118.7, 118.3, 38.1, 31.3, 24.0, 22.4, 13.8. Lit.[40] δ 207.18, 162.70, 136.36, 130.18, 119.53, 119.01, 118.70, 38.49, 31.64, 24.41, 22.67, 14.11. IR: 3426, 1639, 1487, 1447, 1197, 1156, 752. HRMS: (EI) 192.1150 calcd for $C_{12}H_{16}O_2$ (M^+); found 192.1145. Lit.[40] 192.

4.4.3.5. 1-(2-Hydroxyphenyl)-2-phenylethanone (2g). Synthesis was performed using the general procedure described above using **1g** (1.5 g, 7.0 mmol), MnO_2 (6.0 g, 69 mmol), and CH_2Cl_2 (80 mL). Compound **2g** was isolated as a colorless oil (624 mg, 2.94 mmol, 42%). ^1H NMR: ($CDCl_3$) δ 12.27 (s, 1H), 7.86 (dd, $J = 2$ Hz, $J = 8$ Hz, 1H), 7.45 (m, 1H), 7.36 (m, 2H), 7.31 (m, 3H), 6.99 (m, 1H), 6.88 (m, 1H), 4.29 (s, 2H). Lit.[39] δ 12.1 (s, 1H), 7.73–6.91 (m, 9H), 4.2 (s, 2H). $^{13}C\{^1H\}$ NMR: ($CDCl_3$) δ 203.7, 162.7, 136.4, 133.8, 130.3, 129.3, 128.6, 127.0, 118.9, 118.9, 118.5, 44.9. Lit.[39] δ 203.7, 162.7, 136.3–118.4 (11C), 44.9. IR: 1638, 1487, 1446, 1344, 1275, 1156, 754. Lit.[39] 1680. HRMS: (EI) 212.0837 calcd for $C_{14}H_{12}O_2$ (M^+); found 212.0835. Lit.[39] 212.

4.4.4. General procedure for the preparation of compounds 3a–i. A round bottom flask was charged with the appropriate 2′-hydroxyketophenol(**2**), CH_2Cl_2, and cooled to −78 °C. $TiCl_4$ (1.0 M CH_2Cl_2 solution) was added dropwise by syringe and was stirred for 1 h at −78 °C to produce a reddish-brown-colored solution. Diisopropylethylamine was added and the reaction was stirred at −78 °C for 1 h. 4-Dichloromethylenemorpholin-4-ium chloride was added and the reaction mixture was stirred at −78 °C then warmed to 0 °C for 2 h, then allowed to warm to rt and stirred overnight. The reaction mixture was cooled to 0 °C, and Et_3N and MeOH were added. The stirred reaction mixture was allowed to warm to rt over 3 h. The volatile materials were removed in vacuo to give a crude red-colored residue that was washed with $NaHCO_3$ (satd, 30 mL), then the solids were extracted with CH_2Cl_2 (3×15 mL). The combined organics were dried over $MgSO_4$, filtered, and concentrated in vacuo to give a crude oil, which was purified by flash column chromatography, and lyophilized from C_6H_6 to give a flocculent white powder. Characterization of each derivative is described below.

4.4.4.1. 2-Morpholin-4-yl-chromen-4-one (LY292223) (3a). Synthesis was performed using the general procedure described above using 2′-hydroxyacetophenone (565 mg, 4.15 mmol), CH_2Cl_2 (11 mL), $TiCl_4$ (6.5 mL of a 1.0 M CH_2Cl_2 solution, 6.5 mmol), diisopropylethylamine (2.7 mL, 15.5 mmol), 4-dichloromethylenemorpholin-4-ium chloride (1.2 g, 5.0 mmol), Et_3N (1.0 mL), and MeOH (5 mL). Column chromatography: SiO_2, 40% EtOAc–hexanes + 1% Et_3N to 90% EtOAc–MeOH + 1% Et_3N gradient (344 mg, 1.5 mmol, 36%). ^1H NMR: ($CDCl_3$) δ 7.95, 7.35, 7.14, 7.08, 5.27 (s, 1H), 3.63 (t, $J = 5$ Hz, 4H), 3.30 (t, $J = 5$ Hz, 4H). Lit.[40] δ 8.15 (m, 1H), 7.56 (m, 1H), 7.31 (m, 2H), 5.49 (s, 1H), 3.83 (t, $J = 4.7$ Hz, 4H), 3.50 (t, $J = 4.7$ Hz, 4H). $^{13}C\{^1H\}$ NMR: ($CDCl_3$) δ 176.8, 162.5, 153.5, 132.2, 125.2, 124.6, 122.8, 116.3, 87.0, 65.8, 44.5. Lit.[40] δ 176.9, 162.4, 153.5, 132.1, 125.3, 124.6, 122.7, 116.1, 87.2, 65.8, 44.4. IR: 1616, 1555, 1418, 1300, 1251, 1117, 985, 766. Lit.[40] 1622, 1559. HRMS: (EI) 231.0895 calcd for $C_{13}H_{13}NO_3$ (M^+); found 231.0887. Anal. Calcd for $C_{13}H_{13}NO_3$: C, 67.52; H, 5.66; N, 6.00. Found: C, 67.59; H, 5.69; N, 5.97.

4.4.4.2. 3-Methyl-2-morpholin-4-yl-chromen-4-one (3b). Synthesis was performed using the general procedure described above using 200 mg 2′-hydroxypropiophenone, 3.5 mL CH_2Cl_2, 2.0 mmol $TiCl_4$, 600 mg *i*-Pr_2EtN, 308 mg dichloromethylenemorpholin-4-ium chloride, 0.4 mL Et_3N, and 2 mL MeOH. Column chromatography: SiO_2, 50% EtOAc–hexanes + 1% Et_3N (77 mg, 0.31 mmol, 24%). ^1H NMR: (C_6D_6) δ 8.52 (d, $J = 8$ Hz, 1H), 7.07 (m, 1H), 6.93 (m, 2H), 3.31 (t, $J = 5$ Hz, 4H), 2.70 (t, $J = 5$ Hz, 4H), 2.01 (s, 3H). $^{13}C\{^1H\}$ NMR: (C_6D_6) δ 177.9, 161.5, 154.2, 132.0, 126.4, 124.6, 123.4, 116.7, 103.6, 66.5, 48.3, 11.0. IR: 1612, 1556, 1410, 1114. HRMS: (EI) 245.1051 calcd for $C_{14}H_{15}NO_3$ (M^+); found 245.1050. Combustion analysis was not obtained for this compound due to its similarity to **3a–i**.

4.4.4.3. 3-Ethyl-2-morpholin-4-yl-chromen-4-one (3c). Synthesis was performed using the general procedure described above using 407 mg **2c**, 30 mL CH_2Cl_2, 3.71 mmol $TiCl_4$, 3.2 g *i*-Pr_2EtN, 759 mg dichloromethylenemorpholin-4-ium chloride, 0.6 mL Et_3N, and 3 mL MeOH. Column chromatography: SiO_2, 30% EtOAc–hexanes + 1% Et_3N (364 mg, 1.40 mmol, 57%). ^1H NMR: (C_6D_6) δ 8.29 (d, $J = 8$ Hz, 1H), 7.12 (m, 1H), 6.95 (m, 2H), 3.40 (t, $J = 5$ Hz, 4H), 2.83 (t, $J = 5$ Hz, 4H), 2.48 (q, $J = 7$ Hz, 2H), 1.19 (t, $J = 7$ Hz, 3H). $^{13}C\{^1H\}$ NMR: (C_6D_6) δ 177.8, 161.8,

154.2, 132.3, 126.0, 124.5, 123.5, 116.9, 110.4, 66.6, 49.3, 18.6, 13.3. IR: 1615, 1556, 1467, 1401, 1361, 1264, 1223, 1116, 759. HRMS: (EI) 259.1208 calcd for $C_{15}H_{17}NO_3$ (M^+); found 259.1199. Anal. Calcd for $C_{15}H_{17}NO_3$: C, 69.48; H, 6.61; N, 5.40. Found: C, 69.43; H, 6.60; N, 5.36.

4.4.4.4. 2-Morpholin-4-yl-3-propylchromen-4-one (3d). Synthesis was performed using the general procedure described above using 68 mg **2d**, 5 mL CH_2Cl_2, 0.57 mmol $TiCl_4$, 490 mg *i*-Pr_2EtN, 117 mg dichloromethylenemorpholin-4-ium chloride, 0.1 mL Et_3N, and 0.5 mL MeOH. Column chromatography: SiO_2, 20% EtOAc–hexanes + 1% Et_3N (58 mg, 0.21 mmol, 56%). ^1H NMR: (C_6D_6) δ 8.46 (d, $J = 6$ Hz, 1H), 7.08 (m, 1H), 6.94 (m, 2H), 3.38 (t, $J = 5$ Hz, 4H), 2.77 (t, $J = 5$ Hz, 4H), 2.57 (t, $J = 8$ Hz, 2H), 1.77 (tq, $J = 8$ Hz, 2H), 0.99 (t, $J = 8$ Hz, 3H). $^{13}C\{^1H\}$ NMR: (C_6D_6) δ 178.2, 162.0, 154.5, 132.2, 126.5, 124.6, 123.6, 116.8, 110.2, 66.6, 49.4, 27.3, 22.0, 14.7. IR: 1616, 1556, 1467, 1400, 1115, 759. HRMS: (EI) 273.1365 calcd for $C_{16}H_{19}NO_3$ (M^+); found 273.1369. Combustion analysis was not obtained for this compound due to its similarity to **3a**–**i**.

4.4.4.5. 3-Isopropyl-2-morpholin-4-yl-chromen-4-one (3e). Synthesis was performed using the general procedure described above using 150 mg **2e**, 10 mL CH_2Cl_2, 1.24 mmol $TiCl_4$, 1.06 g *i*-Pr_2EtN, 253 mg dichloromethylenemorpholin-4-ium chloride, 0.2 mL Et_3N, and 1.0 mL MeOH. Column chromatography: SiO_2, 20% EtOAc–hexanes + 1% Et_3N (138 mg, 0.50 mmol, 60%). ^1H NMR: (C_6D_6) δ 8.36 (d, $J = 8$ Hz, 1H), 7.01 (m, 1H), 6.89 (m, 2H), 3.47 (t, $J = 5$ Hz, 4H), 2.96 (m, 1H), 2.72 (t, $J = 5$ Hz, 4H), 1.54 (d, $J = 7$, 6H). $^{13}C\{^1H\}$ NMR: (C_6D_6) δ 178.2, 162.1, 154.4, 132.2, 126.3, 124.5, 124.4, 116.7, 115.2, 66.4, 50.1, 27.7, 20.5. IR: 1616, 1557, 1466, 1390, 1217, 1115, 759. HRMS: (EI) 273.1364 calcd for $C_{16}H_{19}NO_3$ (M^+); found 273.1364. Combustion analysis was not obtained for this compound due to its similarity to **3a**–**i**.

4.4.4.6. 3-Butyl-2-morpholin-4-yl-chromen-4-one (3f). Synthesis was performed using the general procedure described above using 375 mg **2f**, 20 mL CH_2Cl_2, 2.92 mmol $TiCl_4$, 2.51 g *i*-Pr_2EtN, 597 mg dichloromethylenemorpholin-4-ium chloride, 0.4 mL Et_3N, and 2.0 mL MeOH. Column chromatography: SiO_2, 20% EtOAc–hexanes + 1% Et_3N (296 mg, 1.03 mmol, 53%). ^1H NMR: (C_6D_6) δ 8.48 (d, $J = 8$ Hz, 1H), 7.07 (m, 1H), 6.93 (m, 2H), 3.39 (t, $J = 5$ Hz, 4H), 2.77 (t, $J = 5$ Hz, 4H), 2.61 (t, $J = 8$ Hz, 2H), 1.75 (p, $J = 8$ Hz, 2H), 1.41 (s, $J = 8$ Hz, 2H), 0.95 (t, $J = 8$ Hz, 3H). $^{13}C\{^1H\}$ NMR: (C_6D_6) δ 178.1, 162.0, 154.5, 132.2, 126.5, 124.6, 123.7, 116.8, 110.4, 66.6, 49.4, 30.8, 24.8, 23.3, 14.2. IR: 1615, 1558, 1466, 1398, 1223, 1116, 759. HRMS: (EI) 287.1521 calcd for $C_{17}H_{21}NO_3$ (M^+); found 287.1520. Combustion analysis was not obtained for this compound due to its similarity to **3a**–**i**.

4.4.4.7. 2-Morpholin-4-yl-3-phenylchromen-4-one (3g). Synthesis was performed using the general procedure described above using 143 mg **2g**, 5 mL CH_2Cl_2, 1.01 mmol $TiCl_4$, 870 mg *i*-Pr_2EtN, 206 mg dichloromethylenemorpholin-4-ium chloride, 0.1 mL Et_3N, and 0.5 mL MeOH. Column chromatography: SiO_2, 20% EtOAc–hexanes + 1% Et_3N (144 mg, 0.47 mmol, 70%). ^1H NMR: (C_6D_6) δ 8.39 (d, $J = 8$ Hz, 1H), 7.47 (m, 2H), 7.20 (m, 2H), 7.11–7.02 (m, 2H), 6.96–6.90 (m, 2H), 3.11 (t, $J = 5$ Hz, 4H), 2.68 (t, $J = 5$ Hz, 4H). $^{13}C\{^1H\}$ NMR: (C_6D_6) δ 175.5, 160.9, 153.6, 134.5, 132.2, 131.3, 128.2, 126.9, 126.6, 124.7, 124.0, 116.6, 105.2, 66.1, 47.8. IR: 1614, 1550, 1417, 1340, 1232, 1116, 760. HRMS: (EI) 307.1208 calcd for $C_{19}H_{17}NO_3$ (M^+); found 307.1206. Combustion analysis was not obtained for this compound due to its similarity to **3a**–**i**.

4.4.4.8. 3-Benzyl-2-morpholin-4-yl-chromen-4-one (3h). Synthesis was performed using the general procedure described above using 1.0 g 2′-hydroxy-3-phenylpropiophenone, 12 mL CH_2Cl_2, 6.63 mmol $TiCl_4$, 2.7 mL *i*-Pr_2EtN, 1.2 g dichloromethylenemorpholin-4-ium chloride, 0.2 mL Et_3N, and 1.2 mL MeOH. Column chromatography: SiO_2, 35% EtOAc–hexanes + 1% Et_3N (552 mg, 1.80 mmol, 41%). ^1H NMR: (C_6D_6) δ 8.18 (d, $J = 8$ Hz, 1H), 7.57 (t, $J = 8$ Hz, 1H), 7.34 (m, 2H), 7.19 (m, 5H), 3.94 (s, 2H), 3.67 (t, $J = 5$ Hz, 4H), 3.28 (t, $J = 5$ Hz, 4H). $^{13}C\{^1H\}$ NMR: (C_6D_6) δ 178.5, 162.8, 153.9, 140.0, 132.6, 128.4, 127.9, 126.1, 125.9, 124.7, 122.6, 116.7, 106.5, 66.6, 48.8, 30.5. IR: 1615, 1555, 1467, 1402, 1236, 1114, 759. HRMS: (EI) 321.1365 calcd for $C_{20}H_{19}NO_3$ (M^+); found 321.1368. Combustion analysis was not obtained for this compound due to its similarity to **3a**–**i**.

4.4.4.9. 3-Decyl-2-morpholin-4-yl-chromen-4-one (3i). Synthesis was performed using the general procedure described above for 102 mg 2′-hydroxydodecanophenone, 3.0 mL CH_2Cl_2, 0.551 mmol $TiCl_4$, 473 mg *i*-Pr_2EtN, 113 mg dichloromethylenemorpholin-4-ium chloride, 0.06 mL Et_3N, and 0.3 mL MeOH. Column chromatography: SiO_2, 20% EtOAc–hexanes + 1% Et_3N. (37 mg, 0.098 mmol, 27%). ^1H NMR: (C_6D_6) δ 8.50 (d, $J = 8$ Hz, 1H), 7.07 (m, 1H), 6.93 (m, 2H), 3.42 (t, $J = 5$ Hz, 4H), 2.80 (t, $J = 5$ Hz, 4H), 2.66 (t, $J = 8$ Hz, 2H), 1.82 (m, 2H), 1.48–1.20 (m, 14H), 0.90 (t, $J = 7$ Hz, 3H). $^{13}C\{^1H\}$ NMR: (C_6D_6) δ 178.2, 162.0, 154.5, 132.2, 126.5, 124.6, 123.7, 116.8, 110.5, 66.6, 49.4, 32.3, 30.4, 30.11, 30.09, 29.9, 29.8, 28.7, 25.2, 23.1, 14.3. IR: 1615, 1561, 1466, 1395, 1117. HRMS: (EI) 371.2460 calcd for $C_{23}H_{33}NO_3$ (M^+); found 371.2458. Combustion analysis was not obtained for this compound due to its similarity to **3a**–**i**.

Acknowledgements

We thank the members of the Shokat research group, particularly Quincey Justman, Scott Lazerwith, Jennifer Paulson, and Daniel Rauh, as well as Professor James Bobbitt (Univ. Connecticut) for helpful discussions. Funding was provided by postdoctoral fellowships from the Susan G. Komen Breast Cancer Foundation and the California Section of the American Cancer Society (P.J.A.), a predoctoral fellowship from the Howard

Hughes Medical Institute (Z.A.K.), NIH grant AI440099 (K.M.S.), and an award from the Sandler Program for Asthma Research (K.M.S.). Mass spectra were provided by the Center for Mass Spectrometry at the University of California, San Francisco, supported by the NIH division of Research Resources.

Supplementary data

Supplementary data associated with this article can be found, in the online version, at doi:10.1016/j.bmc.2005.02.021.

References and notes

1. Blencke, S.; Zech, B.; Engkvist, O.; Greff, Z.; Orfi, L.; Horvath, Z.; Keri, G.; Ullrich, A.; Daub, H. Characterization of a conserved structural determinant controlling protein kinase sensitivity to selective inhibitors. *Chem. Biol.* **2004**, *11*, 691–701.
2. Liu, Y.; Bishop, A.; Witucki, L.; Kraybill, B.; Shimizu, E.; Tsien, J.; Ubersax, J.; Blethrow, J.; Morgan, D. O.; Shokat, K. M. Structural basis for selective inhibition of Src family kinases by PP1. *Chem. Biol.* **1999**, *6*, 671–678.
3. Ward, S.; Sotsios, Y.; Dowden, J.; Bruce, I.; Finan, P. Therapeutic potential of phosphoinositide 3-kinase inhibitors. *Chem. Biol.* **2003**, *10*, 207–213.
4. Ward, S. G.; Finan, P. Isoform-specific phosphoinositide 3-kinase inhibitors as therapeutic agents. *Curr. Opin. Pharmacol.* **2003**, *3*, 426–434.
5. Noble, M. E.; Endicott, J. A.; Johnson, L. N. Protein kinase inhibitors: insights into drug design from structure. *Science* **2004**, *303*, 1800–1805.
6. Druker, B. J. Molecularly targeted therapy: have the floodgates opened?. *Oncologist* **2004**, *9*, 357–360.
7. Druker, B. J.; Tamura, S.; Buchdunger, E.; Ohno, S.; Segal, G. M.; Fanning, S.; Zimmermann, J.; Lydon, N. B. Effects of a selective inhibitor of the Abl tyrosine kinase on the growth of Bcr-Abl positive cells. *Nat. Med.* **1996**, *2*, 561–566.
8. Eyers, P. A.; Craxton, M.; Morrice, N.; Cohen, P.; Goedert, M. Conversion of SB 203580-insensitive MAP kinase family members to drug-sensitive forms by a single amino-acid substitution. *Chem. Biol.* **1998**, *5*, 321–328.
9. Shah, K.; Liu, Y.; Deirmengian, C.; Shokat, K. M. Engineering unnatural nucleotide specificity for Rous sarcoma virus tyrosine kinase to uniquely label its direct substrates. *Proc. Natl. Acad. Sci. U.S.A.* **1997**, *94*, 3565–3570.
10. Blencke, S.; Ullrich, A.; Daub, H. Mutation of threonine 766 in the epidermal growth factor receptor reveals a hotspot for resistance formation against selective tyrosine kinase inhibitors. *J. Biol. Chem.* **2003**, *278*, 15435–15440.
11. Gorre, M. E.; Mohammed, M.; Ellwood, K.; Hsu, N.; Paquette, R.; Rao, P. N.; Sawyers, C. L. Clinical resistance to STI-571 cancer therapy caused by BCR-ABL gene mutation or amplification. *Science* **2001**, *293*, 876–880.
12. Bishop, A. C.; Ubersax, J. A.; Petsch, D. T.; Matheos, D. P.; Gray, N. S.; Blethrow, J.; Shimizu, E.; Tsien, J. Z.; Schultz, P. G.; Rose, M. D.; Wood, J. L.; Morgan, D. O.; Shokat, K. M. A chemical switch for inhibitor-sensitive alleles of any protein kinase. *Nature* **2000**, *407*, 395–401.
13. Liu, Y.; Shah, K.; Yang, F.; Witucki, L.; Shokat, K. M. A molecular gate which controls unnatural ATP analogue recognition by the tyrosine kinase v-Src. *Bioorg. Med. Chem.* **1998**, *6*, 1219–1226.
14. Shah, N. P.; Tran, C.; Lee, F. Y.; Chen, P.; Norris, D.; Sawyers, C. L. Overriding imatinib resistance with a novel ABL kinase inhibitor. *Science* **2004**, *305*, 399–401.
15. La Rosee, P.; Corbin, A. S.; Stoffregen, E. P.; Deininger, M. W.; Druker, B. J. Activity of the Bcr-Abl kinase inhibitor PD180970 against clinically relevant Bcr-Abl isoforms that cause resistance to imatinib mesylate (Gleevec, STI571). *Cancer Res.* **2002**, *62*, 7149–7153.
16. Katso, R.; Okkenhaug, K.; Ahmadi, K.; White, S.; Timms, J.; Waterfield, M. D. Cellular function of phosphoinositide 3-kinases: implications for development, homeostasis, and cancer. *Annu. Rev. Cell Dev. Biol.* **2001**, *17*, 615–675.
17. Samuels, Y.; Wang, Z.; Bardelli, A.; Silliman, N.; Ptak, J.; Szabo, S.; Yan, H.; Gazdar, A.; Powell, S. M.; Riggins, G. J.; Willson, J. K.; Markowitz, S.; Kinzler, K. W.; Vogelstein, B.; Velculescu, V. E. High frequency of mutations of the PIK3CA gene in human cancers. *Science* **2004**, *304*, 554.
18. Leslie, N. R.; Downes, C. P. PTEN function: how normal cells control it and tumour cells lose it. *Biochem. J.* **2004**, *382*, 1–11.
19. Nagata, Y.; Lan, K. H.; Zhou, X.; Tan, M.; Esteva, F. J.; Sahin, A. A.; Klos, K. S.; Li, P.; Monia, B. P.; Nguyen, N. T.; Hortobagyi, G. N.; Hung, M. C.; Yu, D. PTEN activation contributes to tumor inhibition by trastuzumab, and loss of PTEN predicts trastuzumab resistance in patients. *Cancer Cell* **2004**, *6*, 117–127.
20. Cappuzzo, F.; Magrini, E.; Ceresoli, G. L.; Bartolini, S.; Rossi, E.; Ludovini, V.; Gregorc, V.; Ligorio, C.; Cancellieri, A.; Damiani, S.; Spreafico, A.; Paties, C. T.; Lombardo, L.; Calandri, C.; Bellezza, G.; Tonato, M.; Crino, L. Akt phosphorylation and gefitinib efficacy in patients with advanced non-small-cell lung cancer. *J. Natl. Cancer Inst.* **2004**, *96*, 1133–1141.
21. Sordella, R.; Bell, D. W.; Haber, D. A.; Settleman, J. Gefitinib-sensitizing EGFR mutations in lung cancer activate anti-apoptotic pathways. *Science* **2004**, *305*, 1163–1167.
22. Luo, J.; Manning, B. D.; Cantley, L. C. Targeting the PI3K-Akt pathway in human cancer: rationale and promise. *Cancer Cell* **2003**, *4*, 257–262.
23. Walker, E. H.; Pacold, M. E.; Perisic, O.; Stephens, L.; Hawkins, P. T.; Wymann, M. P.; Williams, R. L. Structural determinants of phosphoinositide 3-kinase inhibition by wortmannin, LY294002, quercetin, myricetin, and staurosporine. *Mol. Cell* **2000**, *6*, 909–919.
24. Matter, W. F.; Brown, R. F.; Vlahos, C. J. The inhibition of phosphatidylinositol 3-kinase by quercetin and analogs. *Biochem. Biophys. Res. Commun.* **1992**, *186*, 624–631.
25. Walker, E. H.; Perisic, O.; Ried, C.; Stephens, L.; Williams, R. L. Structural insights into phosphoinositide 3-kinase catalysis and signalling. *Nature* **1999**, *402*, 313–320.
26. Herman, P. K.; Emr, S. D. Characterization of VPS34, a gene required for vacuolar protein sorting and vacuole segregation in *Saccharomyces cerevisiae*. *Mol. Cell Biol.* **1990**, *10*, 6742–6754.
27. Kato, R.; Ogawa, H. An essential gene, ESR1, is required for mitotic cell growth, DNA repair and meiotic recombination in *Saccharomyces cerevisiae*. *Nucleic Acids Res.* **1994**, *22*, 3104–3112.
28. Desany, B. A.; Alcasabas, A. A.; Bachant, J. B.; Elledge, S. J. Recovery from DNA replicational stress is the essential function of the S-phase checkpoint pathway. *Genes Dev.* **1998**, *12*, 2956–2970.

29. Pal, D.; Chakrabarti, P. Beta-sheet propensity and its correlation with parameters based on conformation. *Acta Crystallogr. D Biol. Crystallogr.* **2000**, *56*(Pt. 5), 589–594.
30. Vlahos, C. J.; Matter, W. F.; Hui, K. Y.; Brown, R. F. A specific inhibitor of phosphatidylinositol 3-kinase, 2-(4-morpholinyl)-8-phenyl-4*H*-1-benzopyran-4-one (LY294002). *J. Biol. Chem.* **1994**, *269*, 5241–5248.
31. Knight, Z. A.; Chiang, G. C.; Alaimo, P. J.; Kenski, D. M.; Ho, C. B.; Coan, K.; Abraham, R. T.; Shokat, K. M. Isoform-specific phosphoinositide 3-kinase inhibitors from an arylmorpholine scaffold. *Bioorg. Med. Chem.* **2004**, *12*, 4749–4759.
32. Sadhu, C.; Dick, K.; Tino, W. T.; Staunton, D. E. Selective role of PI3K delta in neutrophil inflammatory responses. *Biochem. Biophys. Res. Commun.* **2003**, *308*, 764–769.
33. Morris, J.; Wishka, D. G.; Fang, Y. A novel synthesis of 2-aminochromones via phosgeniminium salts. *J. Org. Chem.* **1992**, *57*, 6502–6508.
34. Morris, J.; Luke, G. P.; Wishka, D. G. Reaction of phosgeniminium salts with enolates derived from Lewis acid complexes of 2′-hydroxypropiophenones and related beta-diketones. *J. Org. Chem.* **1996**, *61*, 3218–3220.
35. Tanque, Y.; Terada, A.; Seto, I.; Umezu, Y.; Tsuge, O. One-pot ortho hydroxylations of 2-(1-hydroalkyl)naphthylenes and (1-hydroxyalkyl)benzenes. *Bull. Chem. Soc. Jpn.* **1988**, *61*, 1221–1224.
36. Aniol, M.; Wawrzenczyk, C. Chromenes and chromanones. 4. The birch reduction of 2,2-dimethyl-4-chromanone and its 7-substituted analogues. *Heterocycles* **1997**, *45*, 1069–1079.
37. Foster, K. L.; Baker, S.; Brousmiche, D. W.; Wan, P. *o*-Quinone methide formation from excited state intramolecular proton transfer (ESIPT) in an *o*-hydroxystyrene. *J. Photochem. Photobiol. A—Chem.* **1999**, *129*, 157–163.
38. Cimarelli, C.; Palmieri, G. Alkylation of dianions derived from 2-(1-iminoalkyl) phenols: synthesis of functionalized 2-acyl phenols. *Tetrahedron* **1998**, *54*, 15711–15720.
39. Dolhem, E.; Barhdadi, R.; Folest, J. C.; Nedelec, J. Y.; Troupel, M. Nickel catalysed electrosynthesis of ketones from organic halides and iron pentacarbonyl. Part 2: unsymmetrical ketones. *Tetrahedron* **2001**, *57*, 525–529.
40. Morris, J.; Wishka, D. G.; Fang, Y. A cyclodehydration route to 2-aminochromones. *Synth. Commun.* **1994**, *24*, 849–858.